Synthesis and characterisation of material for high-tech agricultural applications

LE NGOC LIEM[a,b,*], DO THANH TIEN[c]
[a]*Faculty of Natural Sciences, Duy Tan University, Da Nang, 550000, Vietnam*
[b]*Institute of Research and Development, Duy Tan University, Da Nang, 550000, Vietnam*
[c]*Faculty of Engineering and Technology, University of Agriculture and Forestry, Hue University, Vietnam*

Luminescent materials, $Ca_2Al_2SiO_7:Ce^{3+}$, Dy^{3+} and $CaAl_2O_4:Mn^{4+}$ were synthesised by solid phase reaction. The red luminescence of $CaAl_2O_4$: Mn^{4+} shows an asymmetric broadband peak at 650 nm corresponding to the characteristic luminescence of Mn^{4+} ions. The luminescent spectra of $Ca_2Al_2SiO_7:Ce^{3+}$, Dy^{3+} phosphors consist of a broadband peak at 420 nm corresponding to the luminescence of Ce^{3+} ions and narrow lines of Dy^{3+} ions. When mixing $Ca_2Al_2SiO_7:Ce^{3+}$, Dy^{3+} and $CaAl_2O_4$: Mn^{4+} materials, the luminescence spectrum was consistent with the absorption maximum of chlorophyll a and chlorophyll b. Therefore, the material could be used in lighting technology for agriculture, tissue culture and transplanting. Moreover, Nano silver solution is synthesized from Paederia foetida L. leaf extract and silver nitrate solution. Nano silver solutions can be used to kill fungus as well as bacteria and to increase the light absorbance of chlorophyll.

(Received August 20, 2020; accepted June 11, 2021)

Keywords: Luminescent, Agricultural lighting, The absorption spectrum of chlorophyll, Nano silver

1. Introduction

The world is facing the risks of climate change, prolonged drought and rapid population growth. Besides that the development of multidrug resistant bacteria, fungi is becoming a severe problem, causing adverse effects on plants, animals, and public health. This leads to increased food shortages in underdeveloped countries. To maintain the nutritional needs of the Earth's people, it is essential to increase the application of high-technology in agricultural production. To boost the production capacity, controlled growing systems using artificial lighting have been considered.

Luminescent material has been studied and applied in technologies in everyday life, such as in optical engineering, lighting technology, cathode ray tubes, signal displays and safety indications [1-6]. Nowadays, luminescent material has many applications in agriculture, such as flowering plant stimulation and low cost fructification. Artificial light has also been used in tissue culture and transplant production technology to create disease-free plant varieties[7]. Currently, fluorescent lamps are typically used for this purpose. However, fluorescent lamps have an emission spectrum ranging from 320 to 800 nm, while the absorption spectrum of chlorophyll ranges from 430 to 450 nm and from 625 to 675 nm[7]. Therefore, it is necessary to find a suitable light source for the absorption spectrum of chlorophyll[8].

Most research on luminescent materials focus on white light emitting diode (LED) synthesis [4], [9-12]. However, luminescent material emitting a wavelength suitable for the chlorophyll absorption spectrum is not extensively researched. Additionally, fungi can cause diseases in plants and lead to low crop yield. To kill fungi, toxic chemicals have been used for a long time. Currently, metallic nanoparticles are being thoroughly explored as potential antimicrobials. Since, AgNPs play vital role in inhibition of microorganisms, it may be used with relative safety for the control of various plant pathogens[7, 13, 14].

In this work, we synthesized two kinds of phosphors namely CAO:Mn^{4+} and CAS:Ce^{3+}, Dy^{3+} by solid phase reaction that are suitable for chlorophyll biosynthesis. Additionally, AgNPs were synthesized eco-friendly and quickly by using the leaves extract of Paederia foetida L. and aqueous solution of silver nitrate, which enhance the absorption of light by plants and play a role in sterilization.

2. Materials and methods

2.1. Preparation of a $CaAl_2O_4$

The $CaAl_2O_4$ (CAO) doped Mn^{4+} ion materials were synthesized by solid state reaction. Commercial powders of with purity of Al_2O_3, B_2O_3, $CaCO_3$, and MnO_2 with purity of 99.9% were use as precursors. These precursors are weighted by molar ratio and mixed with 4 *weight* percent B_2O_3 (used as fluxing agents). The mixtures are well grinded for two hours by using an agate pestle and mortar. Then, the mixtures were anneled at 1250 ºC for 2h in the air environment. The formation of $CaAl_2O_4$: Mn^{4+} is described by following chemical reaction[5]:

$$(1\text{-}x)\ CaCO_3 + Al_2O_3 + x\ MnO_2 \rightarrow Ca_{(1-x)}\ Al_2O_4{:}xMn^{4+} + CO$$

2.2. Preparation of a $Ca_2Al_2SiO_7$

The $Ca_2Al_2SiO_7$ (CAS) co- doped Ce^{3+}, Dy^{3+} ions phosphor were prepared by solid-state reaction. Chemical reagents include: $CaCO_3$ (99.9%, China), Al_2O_3 (99%, China), SiO_2 (99.9%, Korea) and CeO_2 (99.9%, Merck), Dy_2O_3 (99.9%, Merck). These precursors are weighted by molar ratio and mixed with 4 *weight* percent B_2O_3 (used as fluxing agents). The mixtures are well grinded for two hours by using an agate mortar. Then the mixtures were annealed at 1280 ^oC for 1 h in the air environment[6].

The X-ray difraction (XRD) spectra at room temperature were measured by using the diffractometer Bruker D8-Advance at Faculty of Chemistry, Hanoi University of Science. Photoluminescence (PL) and Photoluminescence excitation (PLE) spectra were measured by Flourescent spectrometer FL3-22 Horiba at Duy Tan University, Vietnam. Samples were measured at room temperature and a 450W Xenon lamp was used to excite the sample.

2.3. Preparation of Paederia foetida L. Leaves Extract and Silver Nitrate Solution

Fresh leaves of Paederia foetida L. are shown in Figure 1, were collected from a the garden of the Department of Pharmacy, the Duy Tan University, Vietnam. The leaves collected must be intact and at their prime (neither be too young or too old). Those fresh leaves were then cleaned with fresh water and let air dried by laying them out evenly. 10 g of fresh leaves was obtained, cut into thin strips, then placed into a 200 mL heat-resistant glass flask. Then, they were boiled with distilled water in 5 min, cooled and the mixture was filtered with Whatman filter paper using a vacuum filter[14]. The Paederia foetida L. leaves extract had a light yellow color. The extracted solution was stored in a fridge for further use. Dissolved silver nitrate ($AgNO_3$) from Sigma Aldrich was mixed with distilled water to get 4.10^{-3} M aqueous $AgNO_3$ solution.

Fig. 1. Picture of Paederia foetida L. trees leaves (color online)

3. Results and discussion

3.1. X-ray diffraction of CAO

XRD pattern of CAO: Mn^{4+} (2 mole%) sintered at 1100 ^oC, 1150 ^oC and 1200 ^oC are shown in Fig. 2. Characteristic peaks of $CaAl_2O_4$ with 2θ angle of 22^o, 30^o, 35.5^o, 37.5^o, characteristic peaks of $Ca_9Al_6O_{18}$ at 2θ = 33^o; 59,5^o, of Al_2O_3 at 2θ = 43,4^o, 52,4^o, 57,4^o shows that $CaAl_2O_4$ phase are the dominating phase, the $Ca_9Al_6O_{18}$ phase virtually does not exist. A small amount of doped Mn ions did not affect on the phase composition of based-material $CaAl_2O_4$. The phosphors have the structure of orthorhombic crystal structure and its lattice parameters are a = 8.740 Å, b = 8.100 Å, c = 15.130 Å và $\alpha = \gamma = \beta =$ 90^o . As can be seen, pure monoclinic phase diffraction peaks of parent $CaAl_2O_4$ are dominant in the XRD patterns, and are matching with the JCPDS data file (no. 23-1036)[5, 15].

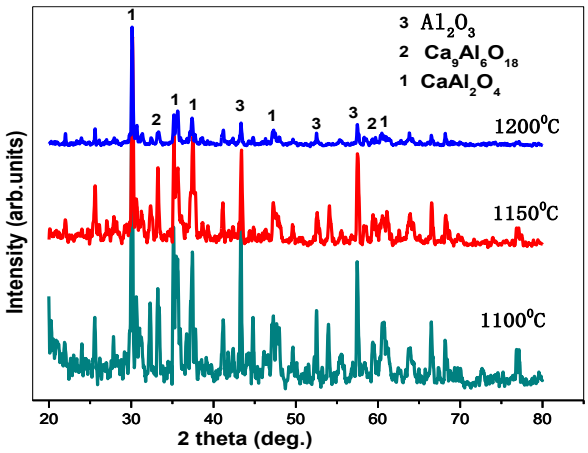

Fig. 2. X-ray diffraction of CAO:Mn^{4+} (2 mole%) (color online)

3.2. X-ray diffraction of CAS

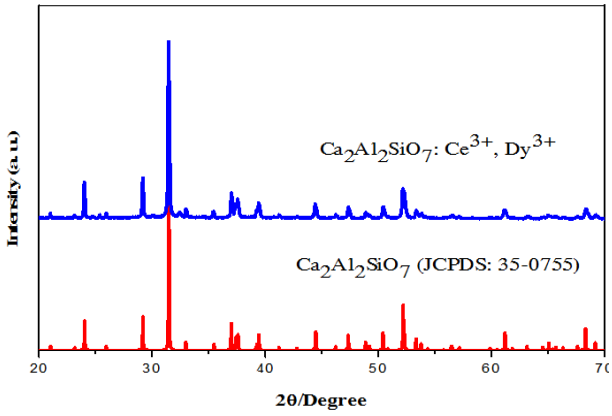

Fig. 3. The XRD diffraction of CAS: Ce^{3+} (0.5 mol%), Dy^{3+} (1 mol%) (color online)

The phosphors of $Ca_2Al_2SiO_7$: Ce^{3+} (0.5 mol%), Dy^{3+} (1 mol%) were successfully synthesized. The crystalline

structure of $Ca_2Al_2SiO_7$: Ce^{3+}, Dy^{3+} were confirmed by X-ray diffraction pattern (XRD) are shown in Fig. 3. The characteristic peaks of the $Ca_2Al_2SiO_7$ were observed. The analysis results show that the samples have tetragonal phase structure, particularly $Ca_2Al_2SiO_7$ with lattice parameters: a = b = 7.69000Å, c = 5.06750Å, α = β = γ = 90°, and space group P-421m ($Ca_2Al_2SiO_7$: JCPDS: 35-0755)[6, 9, 10]. The diffraction diagrams do not show any characteristic peaks of rare earth ions as well as of initial reagent components.

3.3. PL and PLE spectra of CAO: 2%Mn^{4+} samples

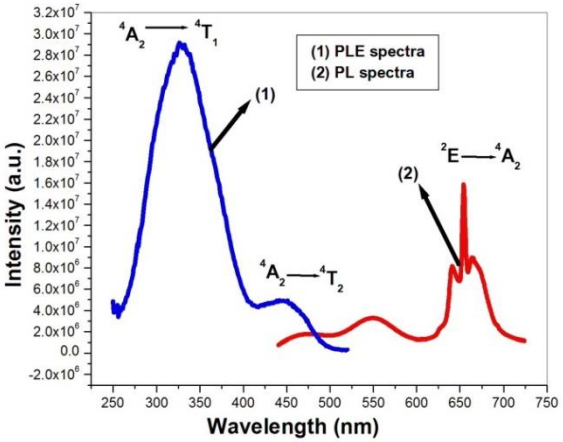

Fig. 4. PL and PLE spectra of CAO:Mn^{4+} phosphor with $\lambda_{ex.}$ = 350 nm for emission and $\lambda_{em.}$ = 650 nm for excitation[5] (color online)

The PL and PLE spectra of CAO: Mn^{4+} are shown in Fig. 4. The PLE spectra with λ_{em} = 650 nm has two broad band with peaks at 450 and 328 nm, correspond to the transition from the ground state $^4A_2$ to excited states $^4T_1$ and $^4T_2$ of Mn^{4+} ions. The PL spectrum with λ_{ex} = 350 nm reveals peaks at 643, 650 and 668 nm which are due to the ^2E to $^4A_2$ states transition of Mn^{4+} ions[16]. In addition, there is a low intensity peak at 545 nm, correspond to the luminescent characteristic of Mn^{2+} because during the synthesis process, some Mn^{4+} ions are reduced to Mn^{2+}[5, 17].

3.4. Photoluminescence properties of CAS: Ce^{3+}, Dy^{3+} phosphors

Fig. 5 shows the PLE and PL spectra of Ce^{3+} and Dy^{3+} single doped and Ce^{3+}, Dy^{3+} codoped in CAS. The PLE spectra of CAS: Ce^{3+} (line 1) monitored at 420 nm exhibits two distinct excitation bands at 275 and 350 nm, which is assigned to the 4f−5d transitions of Ce^{3+}.

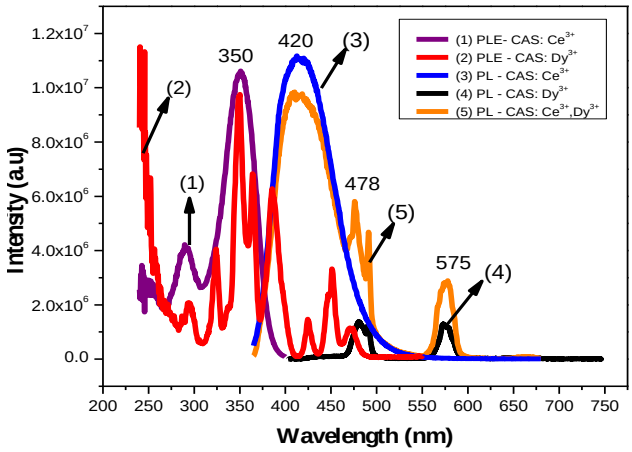

Fig. 5. PLE spectra of CAS: Ce^{3+}(0.5 mol%), λ_{em}=420 nm (1) ,CAS: Dy^{3+} (1.0 mol%), λ_{em}=575 nm (2) and PL spectra with λ_{ex}=350 nm CAS: Ce^{3+}(0.5 mol%) (3), CAS: Dy^{3+}(1.0 mol%) (4), CAS: Ce^{3+}, Dy^{3+}(5) (color online)

Besides, the PL spectrum of Ce^{3+} ions in CAS host lattice (line 3) has a broad band ranging from 365 nm – 525 nm with a maximum at 420 nm, which is attributed to the 5d-4f ($^2F_{5/2}$ and $^2F_{7/2}$) transitions of Ce^{3+}[6, 10], which has high intensity. Meanwhile, the PLE spectrum of CAS: Dy^{3+}(line 2) monitored at 575 nm, shows characteristic narrow lines corresponding to f-f absorption transition of Dy^{3+}, which are appeared at 322 nm, 350 nm, 363 nm, 383 nm, 425 nm, 451 nm[8, 10, 11]. The emission spectrum of CAS: Dy^{3+} shows narrow lines at wavelength 478 nm, 575 nm, corrcorrespond to the state transitions $^4F_{9/2} \rightarrow {}^6H_{J/2}$ (J = 15, 13) of Dy^{3+}[8-10], however their intensity are weaker than that of CAS: Ce^{3+}. From line 3 and line 2 of Fig. 5, that there is an overlap between the emission band of Ce^{3+} and the excitation spectrum of Dy^{3+} indicating the possible resonance type energy transfer from Ce^{3+} to Dy^{3+} ions in the host of CAS. The PL spectra of CAS: Ce^{3+}, Dy^{3+} (line 5) show characteristic peaks of both Ce^{3+} and Dy^{3+}. However, at the same concentration of Ce^{3+} ions, the peak intensity at 420 nm in co-doped is considerably lower than that of single-doped in CAS, while the intensity of peaks correspond to transition of Dy^{3+} are considerably higher than that of single-doped in CAS. As a result, there could exist energy transfer from Ce^{3+} to Dy^{3+} ions in the host of CAS[6].

3.5. Synthesis of Nano-silver material

To this, we mixed 80 mL of $AgNO_3$ solution with 8 mL of Paederia foetida L. leaves extract and divided it into 2 equal portions. The first part called is M_1, the second part called M_2. Then, We put the second portion (M_2) on a shaker machine and stirred for 30 min, 150 rpm at room temperature to synthesize silver nanoparticles (AgNPs)[13]. The first portion (M_1) was heated in a microwave for one minute, operating at a power of 800 W and frequency 2450 MHz to synthesize silver nanoparticles using microwaves (AgNPsmw). Upon microwave irradiation, the colourless solution turned into yellowish-brown indicating the reduction of silver ions

into silver colloids The changed colors of M_1 from light yellow to dark red within one minute in the microwave indicated that the efficiency of (AgNPsmw) synthesis using the microwave assisted method was higher than the non-microwave assisted method[13]. The sample colors are shown in Fig. 6.

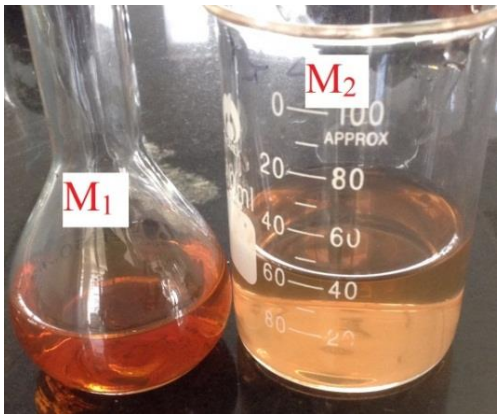

Fig. 6. Photograph of AgNPsmw (M_1) and of AgNPs (M_2) (color online)

The UV-vis spectra (Fig. 7) shows that absorption intensity at around 415 nm of M_1 is higher than that of M_2 and the maximum wavelength of M_1 is smaller than the M_2. Compared with the work of other authors, our study resulted in a smaller particle size, short-time synthesis, and a higher absorption peak intensity.

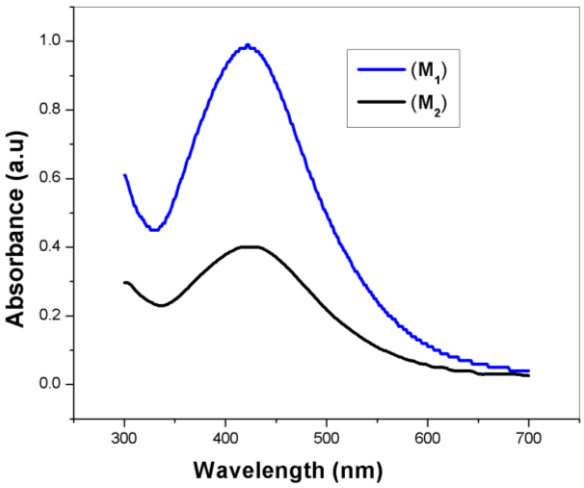

Fig. 7. UV-Vis spectra of AgNPs (M_2), of AgNPsmw (M_1) (color online)

3.5.1. X-ray diffraction (XRD) studies

The structural properties of samples M_1 were studied by XRD and the results are shown in Fig. 8. Four main characteristics of the diffraction peak for Ag were observed at 2θ = 38.2, 44.1, 64.5, and 77.6°, which correspond to the (111), (200), (220) and (311) crystallographic planes of face-centered cubic (fcc) Ag crystals, respectively (JCPDS 00-004-0783)[13, 18].

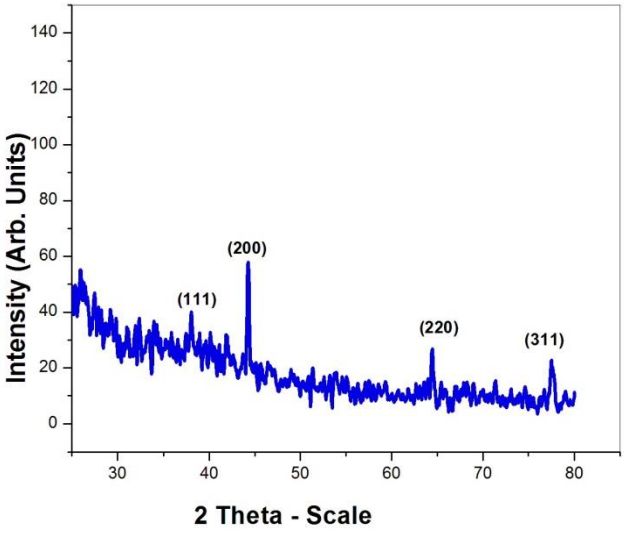

Fig. 8. XRD pattern of AgNps (color online)

3.5.2. Transmission electron microscope (TEM) analysis

The size and shape of the AgNPs was further confirmed by TEM analysis, is shown in Fig. 9. The TEM image of samples M_1 showed particle size about 5 nm. The particle sizes were uniform and no sign of nanoparticle clustering was observed.

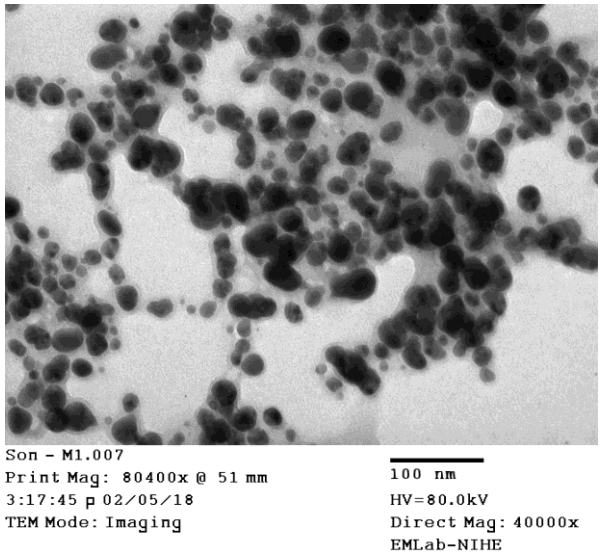

Fig. 9. TEM images of silver nanoparticles

Fig. 10 shows the histogram of size distribution of silver nano particles. Using image analysis software Image J from TEM images, the average particle size measured from the TEM image is less than 5 nm.

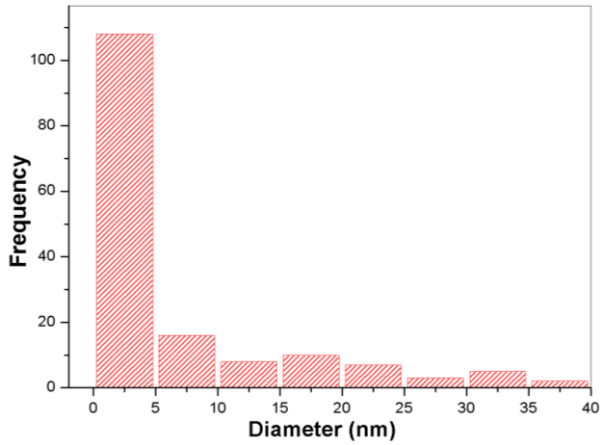

Fig. 10. Histogram showing the particle sizes of AgNPs corresponding to TEM images M_1 (color online)

3.5.3. FT-IR Spectrum

An FT-IR spectrum of silver nanoparticles synthesized by this green method is shown in Fig. 11. A number of absorption peaks at 3261 cm^{-1} and 1637 cm^{-1}. The peaks at 3261cm^{-1} corresponds to O-H and N-H bonds, the peak at 1637cm^{-1} corresponds to the C=O bond, indicating the biomaterial bind to the silver nanoparticles through amine and C=O of amide I and amid II of the protein. These results indicate that Paederia foetida L. leaves extract acts as a reducing and stabilizing agent for silver particles[13, 19].

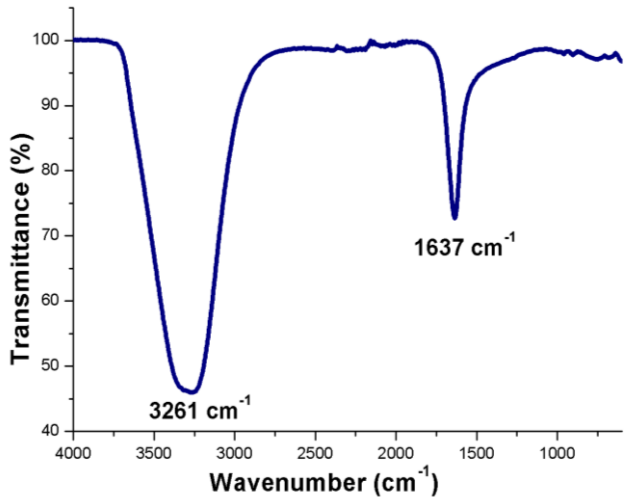

Fig. 11. FTIR spectrum of Paederia foetida L. leaves extract (color online)

3.6. Application of the material in agriculture

Combining the spectra of CAS: Ce^{3+}, Dy^{3+} and CAO: Mn^{4+} material groups, we have two PL spectrum as shown in Figs. 4 and 5 (line red), which shows an asymmetric broadband peak at 420 and 650 nm.

It is known that leaves have two pigment groups, namely chlorophyll a ($C_{55}H_{72}O_5N_4Mg$) and chlorophyll b ($C_{55}H_{70}O_6N_4Mg$), along with a carotenoid auxiliary pigment group ($C_{40}H_{56}$). Chlorophyll a has two absorption maxima around 665 and 430 nm, chlorophyll b has two absorption maxima around 645 and 460 nm, and the auxiliary pigment group has a maximum in the range of 450 to 500 nm[20-22]. According to Thrane, J. E., et al., the leaves have a absorption spectrum as shown in Fig. 12. From the photoluminescence (PL) spectra of CAO: Mn^{4+} (Fig. 4) and CAS: Ce^3, Dy^{3+} (Fig. 5), we can determine that when mixing CAS: Ce^{3+}, Dy^{3+} and CAO: Mn^{4+} material groups, the mixture's PL spectrum shows an overlap with two absorption peaks of chlorophyll a and chlorophyll b. In addition, the maximum at 650 nm overlaps with the absorption spectrum of phytochrome. Therefore, the mixture of the two materials could be applied to light applications in agriculture[16].

The AgNPs material shows an absorption intensity at around 415 nm. Also, the fluorescence emission spectrum of AgNPs has a maximum at 485 nm[23]. From the fluorescence emission spectrum of AgNPs and the absorption spectrum of chlorophyll b and carotenoid, it is seen that there is an overlap between the fluorescence emission spectra of AgNPs and the absorption spectra of chlorophyll b and carotenoid. This may indicate energy transfer from AgNPs to chlorophyll b and carotenoid in leaves. Besides Fungi can cause serious damage in agriculture, resulting in critical losses of yield and quality, the synthesizing silver nanoparticles by Paederia foetida L. leaves extract is eco-friendly and good antimicrobial efficiency against bacteria, viruses, fungi and other microorganisms. Therefore it can be used in high-tech agriculture[24, 25].

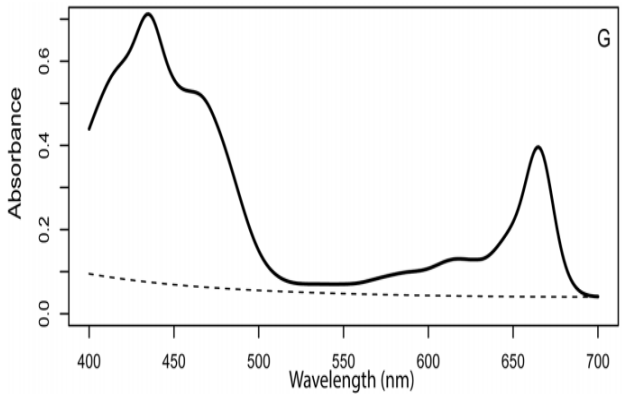

Fig. 12. Absorption spectrum of chlorophyll a/b and carotene[21]

4. Conclusions

In this research, photoluminescent material has been successfully synthesised using a solid phase reaction method, and AgNPs have been synthesised using an eco-friendly method. According to studies by Brian A., Ashenfelter et al. the fluorescence emission spectrum of AgNPs has a maximum at 485 nm. Therefore, fluorescence spectrum of AgNPs overlaps with the absorption spectrum of chlorophyll a/b and carotene. Nano silver particles with particle sizes of 10 to 15 nm, can

penetrate into the leaves while spraying the solution onto them. As the leaves are illuminated by a suitable light, AgNPs particles absorb light before transmitting to the chlorophyll molecules. In addition to enhance the ability of photosynthesis in leaves, AgNPs material can be used to kill fungus as well as bacteria.

The luminescent spectrum of synthesised materials has a wavelength that matches well the absorption wavelength of the chlorophyll a/b. So we concluded that CAS: Ce^{3+}, Dy^{3+} and CAO: Mn^{4+} can be applied to lightning technology in high-tech agricultural applications.

References

[1] G. A. Hebbink, Luminescent Materials based on Lanthanide Ions, Twente University Press, Netherlands, 2002.

[2] Cees Ronda, Luminescence From Theory to Applications, WILEY-VCH Verlag GmbH & Co. KgaA, Weinheim, Germany, 2008.

[3] G. Blasse, B. C. Grabmaier, Luminescent Materials, Springer-Verlag, 1994.

[4] K. Panigrahi, S. Saha, S. Sain, R. Chatterjee, A. Das, U. K. Ghorai, N. Sankar Das, K. K. Chattopadhyay, Dalton Trans **47**(35), 12228 (2018).

[5] L. N. Liem, T. Ngo, IOP Conf. Series **343**, (2018).

[6] D. T. Tien, N. M. Son, L. V. Tuat, L. N. Liem, IOP Conf. Series **540**, (2019).

[7] R. S. Liu, Phosphors, Up conversion Nano Particles, Quantum Dots and their Applications, Springer, 2016.

[8] M. Xia, S. Gu, C. Zhou, L. Liu, Y. Zhong, Y. Zhang, Z. Zhou, RSC Advances **9**, 9244 (2019).

[9] G. Tiwari, N. Brahme, R. Sharma, D. P. Bisen, S. K. Sao, S. J. Dhoble, RSC Advances **6**(55), 49317 (2016).

[10] H. Yiao, Y. Wang, Journal of the Electrochemical Society **156**, 117 (2009).

[11] Y. Gong, Y. Wang, Y. Li, X. Xu, Journal of the Electrochemical Society **157**(6), 208 (2010).

[12] J. Zheng, L. Ying, Q. Cheng, Z. Guo, L. Cai, Y. Lu, C. Chen, Materials Research Bulletin **64**, 51 (2015).

[13] L. N. Liem, N. P. The, N. Dieu, Technologies **7**, (2019).

[14] M. A. Ali, I. Rehman, A. Iqbal, S. Din, A. Q. Rao, A. Latif, T. R. Samiullah, S. Azam, T. Husnain, Adv. life Sci. **1**(3), 129 (2014).

[15] T. Cui, P. Ma, Y. Sheng, K. Zheng, X. Zhou, C. Xu, H. Zou, Y. Song, Optical Materials **67**, 84 (2017).

[16] Z. Zhou, Y. Li, M. Xia, Y. Zhong, N. Zhou, H. T. (Bert) Hintzen, Dalton Trans. **47**, 13713 (2018).

[17] Q. Zhou, L. Dolgov, A. M. Srivastava, L. Zhou, Z. Wang, J. Shi, M. D. Dramićanin, M. G. Brik, M. Wu, J. Mater. Chem. C **6**, 2652 (2018).

[18] V. Manikandan, P. Velmurugan, J. H. Park, W. S. Chang, Y. J. Park, P. Jayanthi, M. Cho, B. T. Oh, Biotech **7**(1), 72 (2017).

[19] M. K. Nahar, Z. Zakaria, U. Hashim, M. F. Bari, Advanced Materials Research **1109**, 35 (2015).

[20] G. Cinque, R. Croce, R. Bassi, Photosynthesis Research **64**, 233 (2000).

[21] J. E. Thrane, M. Kyle, M. Striebel, S. Haande, M. Grung, T. Rohrlack, T. Andersen, PLOS One **10**(9), e0137645 (2015).

[22] Z. Zhou, Y. Zhong, M. Xia, N. Zhou, B. Lei, J. Wang, F. Wu, J. Mater. Chem. C **6**, 8914 (2018).

[23] Z. Parang, A. Keshavarz, S. Farahi, S. M. Elahi, M. Ghoranneviss, S. Parhoodeh, Scientia Iranica **19**, 943 (2012).

[24] M. C. Teixeira, C. Carbone, M. C. Sousa, M. Espina, M. L. Garcia, E. S. Lopez, E. B. Souto, Nanomaterials **10**(3), 560 (2020).

[25] H. Azamal, J. Mohammad, Nanomaterials for Agriculture and Forestry Applications, Elsevier, Amsterdam, Netherlands, 2020.

*Corresponding author: lengocliem@dtu.edu.vn